

# Post-Newtonian $N$ -body simulations

Sverre J. Aarseth <sup>★</sup>

*Institute of Astronomy, Madingley Road, Cambridge CB3 0HA*

Accepted 2007 January XX. Received 2007 January YY; in original form 2007 January 12

## ABSTRACT

We report on the first fully consistent conventional cluster simulation which includes terms up to post<sup>5/2</sup> Newtonian in the potential of the massive body. Numerical problems for treating extremely energetic binaries orbiting a single massive object are circumvented by employing the special “wheel-spoke” regularization method of Zare (1974) which has not been used in large- $N$  simulations before. Idealized models containing  $N = 1 \times 10^5$  particles of mass  $1 M_\odot$  with a central black hole of  $300 M_\odot$  have been studied on GRAPE-type computers. An initial half-mass radius of  $r_h \simeq 0.1$  pc is sufficiently small to yield examples of relativistic coalescence. This is achieved by significant binary shrinkage within a density cusp environment, followed by the generation of extremely high eccentricities which are induced by Kozai (1962) cycles and/or resonant relaxation. More realistic models with white dwarfs and ten times larger half-mass radii also show evidence of GR effects before disruption. Experimentation with the post-Newtonian terms suggests that reducing the time-scales for activating the different orders progressively may be justified for obtaining qualitatively correct solutions without aiming for precise predictions of the final gravitational radiation wave form. The results obtained suggest that the standard loss-cone arguments underestimate the swallowing rate in globular clusters containing a central black hole.

**Key words:** black hole physics – globular clusters: general – methods:  $N$ -body simulations

## 1 INTRODUCTION

$N$ -body simulations of stellar systems containing one or more massive bodies have become popular with a number of studies (Milosavljević & Merritt 2001, Baumgardt, Makino & Ebisuzaki 2004, Baumgardt, Hopman, Portegies Zwart & Makino 2006). This type of work has been inspired by recent determinations of massive black holes (BHs) which reside in galaxies and intermediate mass black holes (IMBHs) have also been considered, particularly in relation to globular clusters. Although the presence of BHs has motivated such work, few papers so far have included the relativistic effects that would be required for an appropriate treatment of deviations from Newtonian motions. One reason for this situation is the numerical challenge of dealing with point-mass dynamics, both as regards the large range in time-scales as well as nearly singular interactions involving superhard binaries. Regularization methods have traditionally been used to overcome problems of this kind. However, existing codes are not tailor-made for dealing with large mass ratios and some attempts to employ two-body (Milosavljević & Merritt 2001) and chain regularization (Szell, Merritt & Mikkola 2005, Amaro-Seoane & Freitag 2006) only succeeded in obtaining modest shrinkage of the dominant binary.

Binary shrinkage by itself is unlikely to be sufficient in achieving relativistic stages for all but the most extreme initial conditions.

Thus, given two BH binary mass components  $m_{\text{BH}} = N^{1/2} \bar{m}$ , where  $\bar{m}$  is the average mass of  $N$  field stars, the final semi-major axis for absorbing half the total energy would be  $4r_h/N$  in terms of the half-mass radius  $r_h$ . Such evolution is well within practical reach for  $N = 10^5$  with present methods. However, this would fall well short of the required shrinkage for relativistic conditions using conventional length-scales. The question therefore arises whether large eccentricities may be generated, thereby reducing the relativistic time-scale significantly by the classical factor  $(1 - e^2)^{7/2}$ .

Results obtained so far have yielded conflicting information about the eccentricity evolution but clues are emerging that this may well depend on initial conditions. An early simulation based on two merging clusters, each containing a massive single object inside a cusp-like system of  $N \simeq 1 \times 10^5$  particles, produced sufficiently large values ( $e_{\text{max}} > 0.995$ ) for the GR coalescence condition (Aarseth 2003b). This work employed the time-transformed leapfrog method (*TTL*) which was specially designed to deal with a massive binary BH (Mikkola & Aarseth 2002) and included the three first post-Newtonian terms. Large eccentricities were also reproduced recently by placing two massive objects inside a single rotating cluster (Berczik et al. 2006). A new study of three massive BHs by direct integration (Iwasawa, Funato & Makino 2006) did achieve coalescence by including relativistic energy loss, albeit for large mass ratios and short times.

Although the binary BH problem is rightly receiving considerable attention, the simpler case of just one massive object is

<sup>★</sup> E-mail: sverre@ast.cam.ac.uk

## 2 Sverre J. Aarseth

still waiting to be explored fully. So far only one major investigation appears to have been directed towards this goal (Preto, Merritt & Spurzem 2004). In this study, the attention was focused on the growth of a density cusp around a massive central object for comparison with Fokker–Planck solutions. In spite of using chain regularization (Mikkola & Aarseth 1993), the maximum growth in  $1/a_{\text{BH}}$  was relatively modest, mainly due to the mass ratio of about 1000 exceeding somewhat the above-mentioned factor of  $N^{1/2}$  for  $N$  in the range  $1 - 2.5 \times 10^5$ .

On the theoretical side, some efforts have been made to look for enhanced relaxation in connection with the loss-cone problem. The interesting concept of resonant relaxation (Rauch & Tremaine 1996) has yet to be tested in large-scale simulations. More recent work (Hopman & Alexander 2006) has hinted at a connection with the Kozai mechanism. On the basis of Fokker–Planck simulations it is suggested that coherent torques change the angular momenta and rotate the orbital inclinations, giving an increased tidal disruption rate for the central region.

The present investigation concentrates on the evolution of the central subsystem using a powerful new implementation. The basic method is a generalization of three-body regularization (Aarseth & Zare 1974) which is of the same vintage (Zare 1974) but apart from one application to four-body scattering (Alexander 1986) has apparently remained dormant. Because of the analogy with spokes on a cart-wheel being connected to the hub, it has been termed “wheel-spoke regularization” (Aarseth 2003a) since each spoke represents mutual interactions with respect to the central hub or reference body. Experience with the three-body regularization code suggests that the extension to arbitrary memberships would make an ideal tool for studying the single BH problem, as was already suggested when the phrase was coined. Such a scheme has the advantage of the massive object acting as a permanent reference body, thereby allowing considerable simplifications compared to the standard chain algorithm. At the same time, post-Newtonian terms are included as perturbations in anticipation of favourable developments for which very high eccentricities would be needed. A full post-Newtonian treatment has already been tried in a different context (Kupi, Amaro-Seoane & Spurzem 2006) for an extremely compact system of 1000 point-mass particles with rms velocity about one percent of the speed of light. The aim here was to study run-away evolution by capture and mergers due to gravitational radiation using two-body regularization, as was first done a long time ago with the code *NBODY5* (Lee 1993) without the precession terms.

This paper begins by outlining the basic method and its implementation in an  $N$ -body system, followed by a description of the initial conditions for an equilibrium distribution. We report on the results of several similar idealized models which illustrate the capabilities of the method. Realistic models which include finite-size effects involving white dwarfs are also considered. Some features of the post-Newtonian implementation are described, with emphasis on the experimental nature of the scheme. Finally a brief discussion is given, together with some suggestions for the future.

## 2 WHEEL-SPOKE IMPLEMENTATION

We begin by defining a subsystem of  $n$  single particles of mass  $m_i$  and one dominant body denoted by  $i = 0$  with mass  $m_0$ . The initial coordinates and momenta in the local centre of mass are given by  $\tilde{\mathbf{q}}_i, \tilde{\mathbf{p}}_i$  for  $i = 0, \dots, n$ . Let us take  $\mathbf{p}_0 = \mathbf{0}$  for the reference body and introduce relative coordinates  $\mathbf{q}_i = \tilde{\mathbf{q}}_i - \tilde{\mathbf{q}}_0$  with respect to

$m_0$ . The Hamiltonian then takes the form

$$H = \sum_{i=1}^n \frac{\mathbf{p}_i^2}{2\mu_i} + \frac{1}{m_0} \sum_{i < j}^n \mathbf{p}_i^T \cdot \mathbf{p}_j - m_0 \sum_{i=1}^n \frac{m_i}{R_i} - \sum_{i < j}^n \frac{m_i m_j}{R_{ij}}, \quad (1)$$

with  $\mu_i = m_i m_0 / (m_i + m_0)$  and  $R_i = |\mathbf{q}_i|$ .

Canonical variables  $\mathbf{Q}_i, \mathbf{P}_i$  with a separable generating function are now introduced for each two-body pair  $m_i, m_0$  by (Zare 1974)

$$W(\mathbf{p}_i, \mathbf{Q}_i) = \sum_{i=1}^n \mathbf{p}_i^T \cdot \mathbf{f}_i(\mathbf{Q}_i), \quad (2)$$

where  $\mathbf{f}_i(\mathbf{Q}_i)$  connects physical and regularized coordinates for spoke index  $i$ . The corresponding regularized momenta take the form

$$\mathbf{P}_i = \mathbf{A}_i \mathbf{p}_i, \quad (i = 1, \dots, n), \quad (3)$$

where  $\mathbf{A}_i$  is *twice* the transpose  $4 \times 4$  Levi–Civita matrix. Inverse transformations yield the relative coordinates and momenta

$$\mathbf{q}_i = \frac{1}{2} \mathbf{A}_i^T \mathbf{Q}_i, \quad \mathbf{p}_i = \frac{1}{4} \frac{\mathbf{A}_i^T \mathbf{P}_i}{R_i}, \quad (4)$$

from which the final physical variables are readily determined. Regularized equations of motion for each spoke interaction are finally obtained by introducing a time transformation. In accordance with standard practice in multiple regularization (Alexander 1986, Mikkola & Aarseth 1993) we adopt the inverse Lagrangian,  $t' = 1/L$ , which has proved effective. Differentiation of the regularized Hamiltonian  $\Gamma^* = t'(H - E_0)$  (where  $E_0$  is the total energy) with respect to  $\mathbf{Q}$  and  $\mathbf{P}$  then yields the equations of motion to be integrated.

The implementation of the wheel-spoke scheme into a general  $N$ -body code requires many special procedures. Quite a few of these can be taken over from other large simulation codes (Aarseth 2003a) when due allowance is made for differences in the data structure. In the following we summarize some of the most relevant features which have much in common with chain regularization.

To begin with, a suitable subsystem must first be chosen for special treatment. The idea here is to select an energetic binary containing the massive BH surrounded only by a small number of perturbers in the central density cusp. The latter requirement invariably implies a relatively small semi-major axis, say  $a_{\text{BH}} \simeq R_{\text{cl}}$ , where  $R_{\text{cl}} \simeq 10r_h/N$  is the adopted close encounter distance for standard regularization treatment. Upon selection of a suitable binary, a few nearby perturbers are added to the new subsystem which is initialized as a composite particle for direct  $N$ -body integration in the usual way (Aarseth 2003a).

Subsequently a variety of heuristic conditions have been employed to control the subsystem size. Particular attention is directed towards limiting the maximum membership because of the  $n(n-1)/2$  force terms which are accumulated by the accurate but time-consuming Bulirsch–Stoer (1966) integrator. Thus the solution method is based on shared but variable time-steps and each step requires many function evaluations for a tolerance of  $10^{-12}$ . Likewise, internal members moving outside a specified distance are removed from the subsystem and play the role as external perturbers while tidal effects are important. The processes of absorbing or emitting subsystem members entails careful updating of the energy budget in order to maintain conservation at a high level.

Particles outside the subsystem also play a role in driving the evolution. External perturbers are selected for distances  $d <$

$[2m_j/m_0\gamma_0]^{1/3} R_{\text{grav}}$ , where  $\gamma_0 = 10^{-6}$  is a small dimensionless parameter measuring the relative perturbation at the boundary and  $R_{\text{grav}}$  is the gravitational radius ( $2a_{\text{BH}}$  for a binary). Since the wheel-spoke formulation only yields regular equations for interactions with the massive body, it is necessary to include a small force softening in the singular terms, thereby permitting the smooth treatment of near-collisions. The softening length was first taken as  $\epsilon = \epsilon_0 R_{\text{grav}}$  with  $\epsilon_0 \simeq 0.01$  and later reduced to  $\epsilon_0 = 0.001$  without experiencing numerical problems. It is updated every time the subsystem is reduced to a dominant binary which occurs frequently. Consistent potential energy corrections are then made at each change in membership. It should be emphasized that softening is only applied between the few non-spoke internal interactions so that the essential dynamics is maintained.

The subsystem solution is combined with the standard Hermite block-step scheme (Makino 1991) which ensures synchronization and consistency. Accordingly, the force on any subsystem perturber is evaluated carefully by summation over all the internal members. The adaptation to special-purpose GRAPE computers is based on the standard *NBODY4* code (Aarseth 2003a) where chain regularization has been bypassed. We note here that possible numerical problems for large mass ratios in chain regularization are circumvented by the present Hamiltonian formulation where the different relative motions are treated on an equal footing. Likewise, the absence of switching and re-initializing the chain for the same membership is beneficial.

A special feature in the present investigation is the addition of post-Newtonian terms in the relativistic regime. This treatment necessitates the introduction of physical units. Scaling to total energy  $E = -1/4$  for the gravitational constant of unity and  $\sum m_i = 1$  gives an rms velocity of  $2^{1/2}/2$  and velocity unit  $V^*$  in  $\text{km s}^{-1}$  once the total mass and length scale is specified. Hence the speed of light is given by  $c = 3 \times 10^5/V^*$  in model units. The resulting equation of motion can be written in a convenient form by (Blanchet & Iyer 2003, Mora & Will 2003)

$$\frac{d^2\mathbf{r}}{dt^2} = \frac{M}{r^2} \left[ (-1 + A) \frac{\mathbf{r}}{r} + B\mathbf{v} \right], \quad (5)$$

where the scaled quantities  $A$  and  $B$  represent the accumulated relativistic effects associated with the separation vector  $\mathbf{r}$  and relative velocity  $\mathbf{v}$ . The latter is readily obtained from the momentum transformations when due allowance is made for the non-zero momentum of  $m_0$  in the local frame.

In the present formulation the perturbing *force* is required for consistency with the equations of motion (cf. Mikkola & Aarseth 1993). Consequently, the desired expression for the dominant two-body motion takes the form

$$\mathbf{F}_{\text{GR}} = \frac{m_i m_0}{c^2 r^2} \left[ \left( A_1 + \frac{A_2}{c^2} + \frac{A_{5/2}}{c^3} + \frac{A_3}{c^4} \right) \frac{\mathbf{r}}{r} + \left( B_1 + \frac{B_2}{c^2} + \frac{B_{5/2}}{c^3} + \frac{B_3}{c^4} \right) \mathbf{v} \right]. \quad (6)$$

In view of the increasing number of operations involved for the higher orders, it is of interest to implement an efficiency scheme depending on time-scale and order. Such an experimental approach aims at providing a qualitative description of the inspiralling process without any predictions for the final coalescence event.

The classical time-scale for radiation energy loss is employed for decision-making purposes. In  $N$ -body units the instantaneous value,  $a/\dot{a}$ , for a large mass ratio is given by (Peters 1964)

$$\tau_{\text{GR}} \simeq \frac{5a^4 c^5}{64m_i m_0^2} \frac{(1-e^2)^{7/2}}{g(e)}, \quad (7)$$

where  $g(e)$  is a known function ( $\simeq 4.5$  for  $e = 1$ ). Provided the time-scale falls below a specified value, the radiation terms  $A_{5/2}$  and  $B_{5/2}$  are added to any Newtonian perturbations for the dominant interaction. Other terms are activated progressively on subsequent reduction of  $\tau_{\text{GR}}$ . Moreover, comparisons with the full scheme for a nearly isolated binary with circular or eccentric orbit yield final coalescence times in essential agreement. Energy conservation is monitored by separate integration of the post-Newtonian perturbation according to

$$\Delta E_{\text{GR}} = \int \mathbf{F}_{\text{GR}} \cdot \mathbf{v} dt, \quad (8)$$

converted to the appropriate regularized form (Mikkola & Aarseth 1993). Note that satisfactory conservation does not guarantee the solution here and is merely a consistency check; hence comparison with known two-body solutions should be carried out.

Since the present full formulation is applicable for quite large deviations from Newtonian dynamics we define GR coalescence in the traditional way as three Schwarzschild radii by

$$r_{\text{coal}} = \frac{6(m_i + m_0)}{c^2}, \quad (9)$$

or about  $8 \times 10^{-10}$  in  $N$ -body units for the standard parameters. This represents over five orders of magnitude in distance range with respect to the initial close encounter length scale,  $R_{\text{cl}}$ .

### 3 INITIAL CONDITIONS

Each simulation project requires careful considerations concerning the initial conditions. In the present work, the introduction of a massive central body may have a significant effect on other nearby particles. Since the emphasis is on studying the evolution of the innermost part, it is desirable to start with an approximate equilibrium distribution. Following an earlier formulation (Aarseth 2003b), we adopt a cusp-like stellar density profile

$$\rho(r) = \frac{1}{r^{1/2}(1+r^{5/2})}. \quad (10)$$

Given a central body of mass  $m_0$ , the corresponding 1D velocity dispersion is generated by (Zhao 1996)

$$\sigma^2(r) = \frac{1}{\rho(r)} \int_r^\infty \frac{\rho(r)}{r^2} [m(r) + m_0] dr, \quad (11)$$

where  $m(r)$  is the enclosed mass within  $r$ .

Several models with  $N = 1 \times 10^5$  equal-mass particles of  $1 M_\odot$  are studied. Based on the discussion above, we take the BH mass as  $N^{1/2} \bar{m}$  which corresponds to  $m_0 = 3 \times 10^{-3}$  in  $N$ -body units with  $m_i = 1 \times 10^{-5}$ . This mass ratio is relatively modest compared to typical values of  $m_{\text{BH}} \simeq 0.01$  used in many investigations of massive binary components.

The choice of total mass and half-mass radius determines the scaled speed of light in the simulation and hence the influence of any post-Newtonian interactions. Since this investigation is a first attempt to evaluate the code performance, standard star cluster parameters would appear to be outside the likely range of interest unless exceptionally large eccentricities are reached. For this reason we first adopt a more conservative length scale of 0.1 pc which yields an initial half-mass radius  $r_h = 0.094$  pc. With the velocity scaling  $V^* \simeq 66 \text{ km s}^{-1}$ , this makes  $c \simeq 4600$  in  $N$ -body units. Consequently, an energetic binary with semi-major axis  $a \simeq 3 \times 10^{-5}$  would need an eccentricity exceeding 0.99 for the radiation time-scale to fall below 400  $N$ -body units which might be

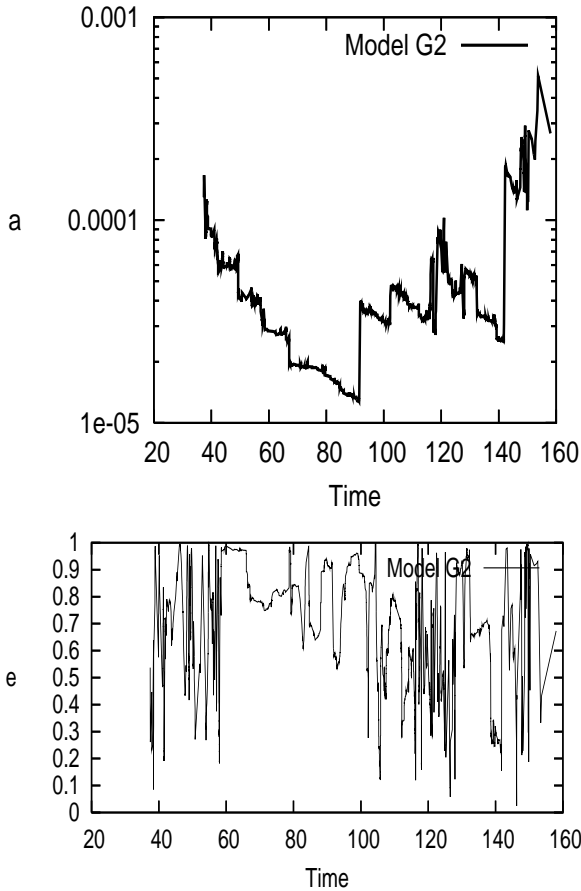


**Figure 1.** Semi-major axis and eccentricity as functions of time, model G2. GR coalescence occurred at  $t = 92, 104, 117, 120, 130, 144, 152$ .

a reasonable criterion for initiating the post-Newtonian treatment since most simulation times are considerably shorter. This compares to the smallest initial central binary of size  $a = 2.5 \times 10^{-4}$  in a typical model and only one more below  $1 \times 10^{-3}$ . Hence a significant evolution is required to achieve a factor of 10 shrinkage of the most energetic binary, especially bearing in mind the increased central velocity dispersion associated with the massive body.

The early cluster evolution exhibits small departures from overall equilibrium as defined by the virial energy ratio. Likewise, the number of particles inside the innermost fixed radii do not show significant changes, in accordance with expectations for an equilibrium model.

Several models assume that the interactions are between point-mass particles. However, it is also of interest to study finite-size objects. The possibility that stars are disrupted by the BH adds another complication. We introduce the tidal disruption distance (Magorrian & Tremaine 1999),

$$r_t = \left( \frac{m_0}{m_i} \right)^{1/3} r^*, \quad (12)$$

and adopt  $r^* = 5 \times 10^{-5}$  au for white dwarfs of  $1 M_\odot$ . In these models, any star inside this distance is removed from the calculation and its mass added to the BH instantaneously. The question of whether such orbits may be modified by post-Newtonian effects before disruption depends on the cluster parameters.

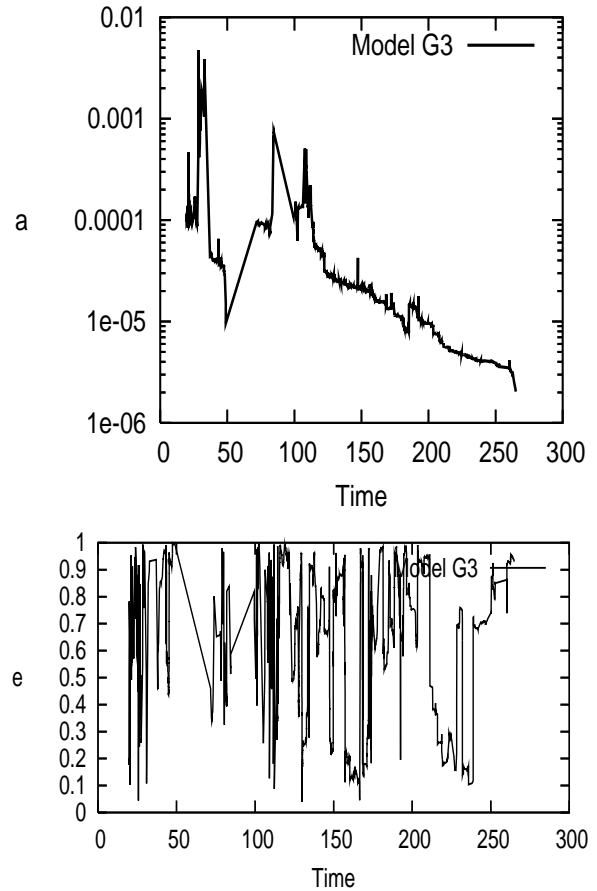


**Figure 2.** Semi-major axis and eccentricity as functions of time, model G3. Coalescence took place at  $t = 22, 30, 50, 84, 104, 186$ .

#### 4 NUMERICAL RESULTS

We first present some results for idealized models which have been studied over at most a few hundred  $N$ -body time units and is sufficient to illustrate the general behaviour. Figure 1 displays the semi-major axis of the innermost bound orbit in model G2 ( $r_h = 0.09$  pc), together with the corresponding eccentricity. Since there are seven GR coalescence events, the downwards trend of the semi-major axis is replaced by the next most strongly bound orbit, whereupon the shrinkage continues. Inspection of the eccentricity graph reveals a number of spikes, with both high and low values which are the hall-mark of Kozai cycles. The growth in eccentricity preceding significant GR radiation loss can be substantial, with pre-relativistic values exceeding  $e \simeq 0.99999$  on several occasions. Likewise, the associated predicted maxima are often very close to unity when the inclination is near  $90^\circ$ . However, not all such configurations are sufficiently stable for GR conditions to develop.

The second model (G3), shown in Fig. 2, exhibits a different behaviour of the smallest semi-major axis, this time with six inspiralling events. Note that during two epochs ( $t \simeq 50 - 70$  and  $86 - 98$ ) the central subsystem is too weakly bound for the special treatment. After an irregular early phase there is a downward trend which is barely affected by the last coalescence. At termination the semi-major axis decreased below the last plotting point to  $1.2 \times 10^{-6}$  and would soon have satisfied the coalescence criterion. During the non-relativistic stage the innermost semi-major axis tends to shrink as a consequence of dynamical evolution. How-

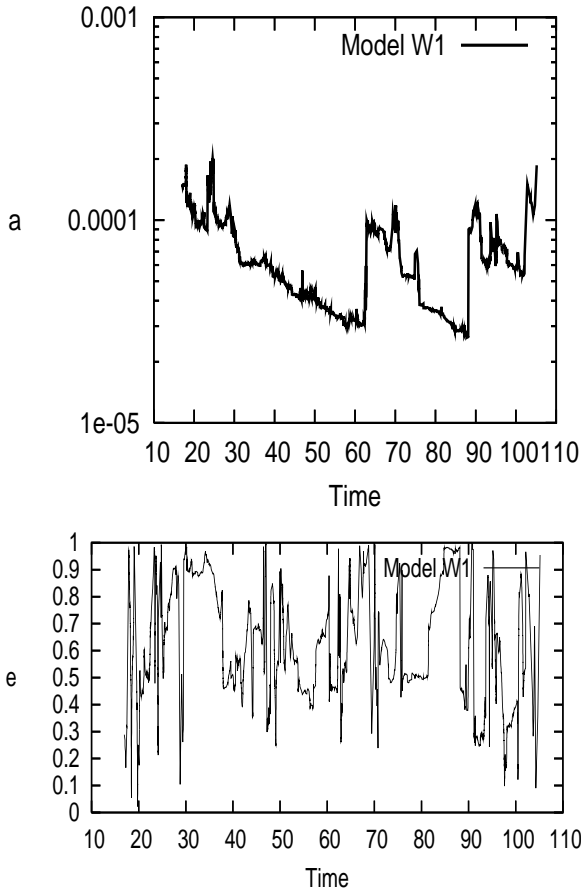


**Figure 3.** Semi-major axis and eccentricity as functions of time, model W1. Disruption occurred at  $t = 25.0, 62.8, 70.2, 88.2, 95.2, 102.5, 104.8$ .

ever, the shrinkage would progress much further but for the large eccentricity which therefore places a lower limit on the period before the GR effect intervenes. Each coalescence is associated with a substantial loss of radiation energy with an accumulated value  $\Delta E_{\text{GR}} \simeq -181$ , consistent with the final Newtonian binding energies. This may be compared with a small systematic drift of  $-2 \times 10^{-5}$  units in the total energy which should be conserved.

These early models employ the point-mass assumption as in most current work. Based on the promising experience gained for point-mass particles it is worth while to enlarge the investigation and include finite-size objects. Given the uncertain status of neutron star populations in globular clusters, it may be more appropriate to consider white dwarfs which should be present with significant abundance in the cores. Since the code can handle a general stellar distribution at a specified age, a study of more realistic mass functions will be undertaken in due course.

In the second set of models, the field stars are taken to be white dwarfs with the characteristic radii and masses quoted above. For continuity we begin with a similar cluster half-mass radius of 0.09 pc (model W1). Figure 3 gives the smallest semi-major axis as a function of time, together with the corresponding eccentricity. There are seven disruptions in this interval, with the relevant times quoted in the figure caption. All but one of these events show significant GR energy loss while the exception is a head-on collision with large pre-relativistic eccentricity,  $e = 0.999999$ . After the seventh disruption, the accumulated relativistic energy was

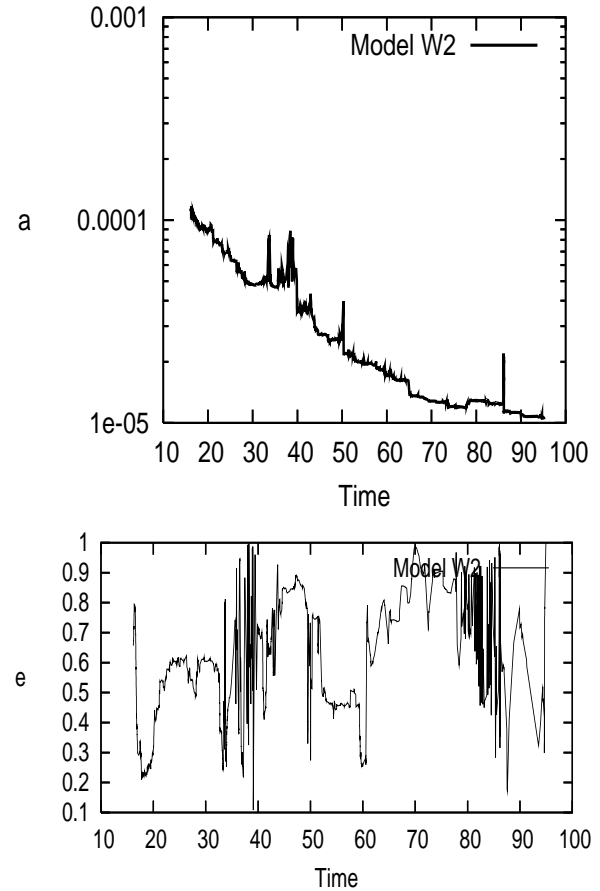


**Figure 4.** Semi-major axis and eccentricity as functions of time, model W2. In this model there was just one disruption at the end.

$\Delta E_{\text{GR}} \simeq -0.31$  which exceeds the initial cluster energy. Once again the eccentricity plot reveals the characteristic spikes associated with Kozai cycles. Note that the corresponding time-scales are sometimes shorter than the plotting intervals so that fine structure is often missing.

The cluster half-mass radius was also varied in order to explore the length-scale dependence. First, a large half-mass radius with  $r_h = 2.8$  pc was chosen for model W2. This gives a smaller disruption radius of  $r_t \simeq 5 \times 10^{-10}$  compared to  $1.6 \times 10^{-8}$  above. The results shown in Fig. 4 contain just one disruption at a comparable time to Fig. 3 ( $t_f \simeq 95$ ). Again a Kozai cycle was apparent, with  $e_{\text{max}} \simeq 0.9998$ . A rather long period of circularization then took place before termination ( $e = 0.1, r = 5 \times 10^{-10}$ ). Until this time, the previously accumulated relativistic energy loss was small which indicates that no other critical approaches were present.

In the final model W3 a cluster of intermediate half-mass radius  $r_h = 0.9$  pc was studied. A collision with small *predicted* pericentre for a wide orbit ( $a \simeq 0.02, 1 - e = 10^{-7}$ ) occurred during the early stage before the compact subsystem formation. All the five disruption events exhibited maximum eccentricities exceeding 0.9999 shortly before termination, evaluated at a non-relativistic distance  $r \simeq 10^{-5}$ . Moreover, in each case the energy loss by equation (8) yielded an amount  $\Delta E_{\text{GR}} \simeq -0.5$ . This shrinkage corresponds to a semi-major axis  $a_{\text{GR}} \simeq 3 \times 10^{-8}$  which agrees with the Newtonian value obtained just before the final plunge.

The density distribution in the central region is also of in-

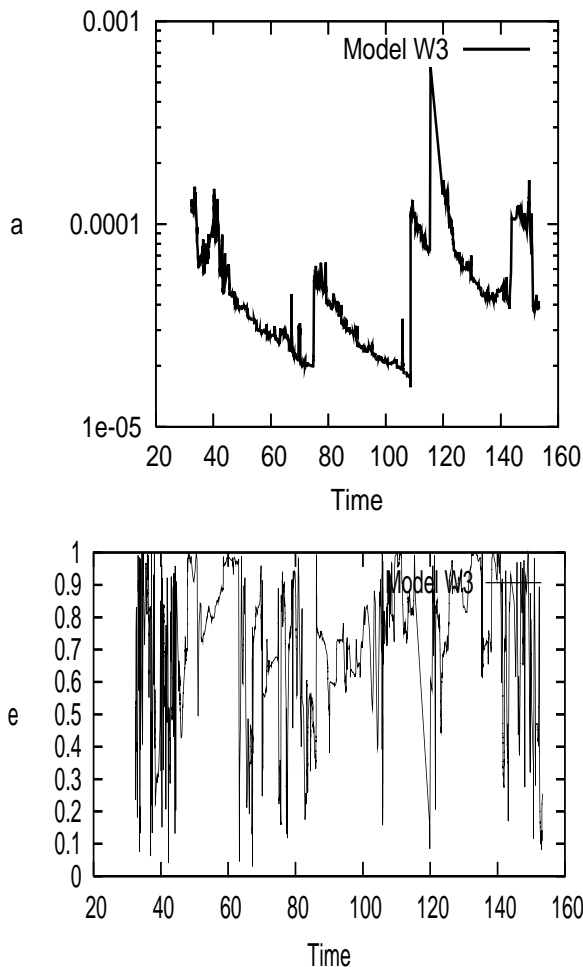


**Figure 5.** Semi-major axis and eccentricity as functions of time, model W3. Five disruption events occurred at  $t = 38.7, 75.0, 108.6, 115.6, 143.8$ .

terest. At typical advanced stages of inner binary evolution ( $a \simeq 2 \times 10^{-5}$ ), there are only about 10 members inside a distance of  $300a$ . Moreover, the second innermost semi-major axis tends to be well separated from the innermost one, thereby giving opportunities for favourable Kozai cycles. Only a few of the dozen or so most extreme eccentricity excursions result in significant energy loss and may therefore be considered rare events.

## 5 POST-NEWTONIAN ASPECTS

The results presented above show examples of relativistic effects leading to coalescence or disruption. Although the inner binary shrinkage is often considerable, the eccentricity plays a key role in initiating the relativistic stage. The process by which large eccentricities are attained is mainly due to third-body secular perturbations known as Kozai (1962) cycles. This requires the perturber to remain in a long-lived orbit around the innermost binary with initial inclination exceeding about  $40^\circ$ . Conservation of angular momentum yields a relation connecting the inclination and inner eccentricity in the form  $\cos^2\theta(1 - e^2) = \text{const}$ . The period for the induced inner eccentricity variation is given by

$$T_{\text{Kozai}} = \frac{T_{\text{out}}^2}{T_{\text{in}}} \left( \frac{1 + q_{\text{out}}}{q_{\text{out}}} \right) (1 - e_{\text{out}}^2)^{3/2} f(e_{\text{in}}, \omega_{\text{in}}, \psi), \quad (13)$$

where  $q_{\text{out}} = m_2/(m_1 + m_0)$  is the mass ratio for the outer orbit with elements  $a_{\text{out}}$ ,  $e_{\text{out}}$  and the function  $f$  which depends on orbital elements is usually of order unity (Heggie 1996).

An expression is also available for the maximum eccentricity of the inner orbit,  $e_{\text{max}}$ , which is of considerable interest (Heggie 1996). Since the period ratio  $T_{\text{out}}/T_{\text{in}}$  may be taken of order 10 for a long-lived system here, this gives  $T_{\text{Kozai}} \simeq 3000T_{\text{out}}(1 - e_{\text{out}}^2)^{3/2}$ . Hence a Kozai period of about  $1000 T_{\text{out}}$  may suffice for  $e_{\text{out}} \simeq 0.7$  and a moderately high inclination, which is frequently seen in such simulations.

A new decision-making scheme has been developed to introduce the different post-Newtonian terms for separate time-scales. Although these terms are increasing in complexity, this is done only partly for computational efficiency. The idea of considering the additional perturbations progressively (Aarseth 2003b) has also been tested by a stand-alone code for the three-body problem<sup>1</sup> (Aarseth & Zare 1974). In the present work, the emphasis is on achieving a qualitatively correct description of the evolution towards coalescence or tidal disruption without aiming for detailed predictions.

Since the main decision-making is based on the two-body elements  $a$  and  $e$ , it is desirable to use relativistic definitions when appropriate. This procedure was not adopted for most of the work reported here. However, the elements are usually evaluated *outside* the semi-major axis of predominantly highly eccentric orbits where GR effects are negligible. For a given level of post-Newtonian implementation, we add the relevant contributions from the two first  $A$  and  $B$  terms of equation (6) according to the relativistic expansion (Mora & Will 2003). Without these corrections, the classical elements show a range of values depending on orbital phase and  $v/c$ . Now the modified two-body energy and angular momentum yield consistent values of the osculating semi-major axis and eccentricity, as can be verified by the available three-body code for an isolated binary. We remark that the relativistic contributions for the white dwarf models are fairly modest, with typical values  $v/c \simeq 4 \times 10^{-4}$  for  $r > a$  near disruption in the case  $r_h = 0.9$  pc.

In the case of a binary we define appropriate time-scales for activating the perturbations in terms of the instantaneous radiation time-scale,  $\tau_{\text{GR}}$ . Thus the radiation term 2.5PN is already included for  $\tau_{\text{GR}} < 1000$   $N$ -body units. The subsequent terms 1PN, 2PN and 3PN are then activated below the experimental values of 100, 50 and 10, respectively. Likewise, the relevant terms are excluded for increasing time-scales up to  $\tau_{\text{GR}} > 2000$  for the GR radiation, with slightly more generous limits being applied in order to prevent repeated switching. Three-body tests show that the final coalescence times for close binaries of different eccentricity are in essential agreement with the full scheme when criteria of this type are employed for a range of parameters. Regarding the choice of boundary values for different levels, the nominal time-scale exceeds the actual coalescence time for circular orbits by a small factor depending on  $c$  due to the loss of angular momentum. At some advanced stage, it may be justified to adopt the unperturbed two-body approximation (Peters 1964) or even define premature termination in order to speed up the calculation.

The possible presence of Kozai cycles adds a further complication since the precession terms act to de-tune the resonance. In particular, the classical ‘‘Mercury’’ precession gives rise to a pericentre advance in radians per orbit,

<sup>1</sup> See the public three-body regularization code TRIPLE3 at <http://www.ast.cam.ac.uk/~sverre/multireg>.

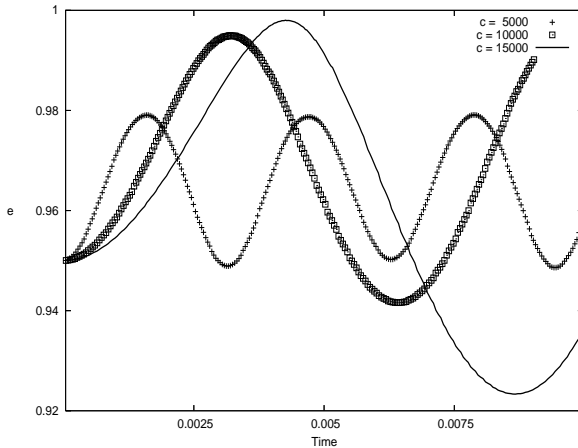


**Figure 6.** Eccentricity as function of time for three values of  $c$ . The elements of the hierarchical three-body configuration are defined in the text.

$$\Delta\omega = \frac{6\pi m_0}{c^2 a (1 - e^2)}, \quad (14)$$

which may be substantial for some conditions of interest. Unless existing post-Newtonian perturbations are present due to a sufficiently short radiation time-scale, the first and second-order precessions are introduced for  $T_{\text{Kozai}} < 10$ . Thus for an eccentric binary with  $e = 0.99$  the precession condition gives  $\Delta\omega \simeq 0.01$  for a typical inner binary of size  $a = 1 \times 10^{-5}$  which is usually covered by either of these criteria. More extreme stages may give rise to a faster advance which is reflected in a shortening of the time-steps. The basic three-body code, which contains identical post-Newtonian expressions to the full code, was used to compare the pericentre advance in the case of strong relativistic effects while suppressing the higher order terms. Here we employed an algorithm measuring the angle between successive apocentre turning points which gave good agreement with equation (14) and therefore provides an independent check on the first-order solution.

Two small bodies orbiting a much heavier one in relative isolation may be sufficiently stable for Kozai cycles to be induced. All that is required is that an outer orbit increases its energy and has a favourable inclination for large eccentricity growth. As has been noted above, this process is seen at later stages when the inner core has been partially depleted. Hence it appears that the final orbital shrinkage before relativistic effects become important is closely correlated with the Kozai resonance. However, the process by which the second most energetic binary migrates inwards in the excavated core and sometimes acquires a large inclination (near 90°) needs to be investigated further.

Idealized Kozai cycles may be studied by the three-body regularization code which employs the same GR terms. Figure 6 illustrates the behaviour of the inner eccentricity for a long-lived hierarchical triple with initial inclination near 90° using  $c = 5000, 10000, 15000$  to represent different mass or length scales. Simulation mass units are adopted with  $a_0 = 1 \times 10^{-5}$ ,  $a_1 = 4.5 \times 10^{-5}$  and eccentricities  $e_0 = 0.95$ ,  $e_{\text{out}} = 0.2$ . From these parameters,  $e_{\text{max}} = 0.9999$  while the peak at 0.9980 is reached for  $c = 15000$ , with  $c$  similar to model W3. This may be sufficient for GR shrinkage to be achieved on a longer time-scale. In this example, the peak eccentricity is maintained over  $\simeq 100$  Kozai cycles with pericentre advance  $\Delta\omega \simeq 0.006$  radians per orbit, and

the slope of the radiation energy loss corresponds to an inspiralling time  $a/\dot{a} \simeq 100$ . The basic Kozai period is a factor of 5 shorter than given by equation (13). Comparison with an earlier analysis (Miller & Hamilton 2002, eq. 6) may also be of interest. We obtain  $\theta_{\text{PN}} \simeq 0.29$  for the dimensionless post-Newtonian Hamiltonian in the realistic example. Although consistent, the expression  $e_{\text{max}} = 1 - \theta_{\text{PN}}^2/9$  applies to the restricted three-body problem.

In a second example,  $a_0 = 5 \times 10^{-5}$ ,  $a_1 = 2.3 \times 10^{-4}$ , with  $c = 15000$  and inclination 100°. Here the inner semi-major axis shrank to  $\simeq 1 \times 10^{-5}$  after some  $3 \times 10^4$  outer periods. During the early stage, up to  $a_0 \simeq 3 \times 10^{-5}$ , the eccentricity was maintained near 0.999 as the result of competition between the Kozai cycle and relativistic decay. This was eventually superseded by pure decay consistent with the analytical expression for  $\dot{e}$  (Peters 1964).

The case of hyperbolic encounters with the BH has been considered in a few simulations only. For this purpose we introduce the capture radius (Quinlan & Shapiro 1989),

$$r_{\text{cap}} = b \left[ \frac{m_0 m_i (m_0 + m_i)^{3/2}}{c^5 v_{\infty}^2} \right]^{2/7}, \quad (15)$$

where  $b = 2.68$  and  $v_{\infty}$  is the velocity at infinity in  $N$ -body units. With the present parameters in the standard white dwarf model we obtain  $r_{\text{cap}} \simeq 9 \times 10^{-9}$  for a typical excess velocity in the core  $v_{\infty} = 1$  and hence capture due to gravitational radiation is not likely to occur before disruption. On the other hand, the capture process is quite feasible in the point-mass case.

## 6 DISCUSSION

The work presented in this paper should be considered exploratory. Although the post-Newtonian formulation itself is well known, a practical implementation presents many additional problems. The attempt to introduce a scheme based on different time-scales without sacrificing essential dynamics appears to have been successful. Likewise, the numerical challenges facing the new implementation have been resolved. Thus it has been demonstrated that the GRAPE-6 combined with the wheel-spoke regularization code is suitable for studying stellar systems with  $10^5$  members and an intermediate massive single BH. A closer analysis of the performance shows that the overheads connected with the central subsystem represent less than 10 per cent (for 64-bit operating system on GRAPE-6A) which is a small price for an accurate treatment. The surprisingly short time-scale for interesting developments also means that significant results can be obtained in a few days even with the smaller GRAPE-6A.

One advantage of using a multiple regularization method, as opposed to the two-body formulation of *NBODY6* (Aarseth 2003a), is that the complicated derivatives of the GR terms are not required (cf. Kupi et al. 2006). On the other hand, it appears that the slight defect of introducing a small softening between the low-mass members of the subsystem is justified<sup>2</sup> (and even smaller values may be acceptable). So far, the 3PN terms have been added for the shortest time-scales,  $\tau_{\text{GR}}$ . This was done for illustrative purposes and may not be required since the 1PN and 2PN terms act to de-tune the Kozai resonance. Contributions from the 3.5PN terms would in principle give rise to a recoil velocity; however, this is likely to be very small for the present mass ratio.

<sup>2</sup> A scaled softening  $\epsilon_0 = 0.001$  and  $R_{\text{grav}} \simeq 10^{-5}$  would correspond to a white dwarf radius in model W3.

So far tidal capture and oblateness effects have not been included (Mardling & Aarseth 2001). General considerations suggest that this process would tend to increase the supply of stars into the loss-cone. On the technical side, the implementation would be more complicated. Thus with two-body regularization it is convenient to apply the orbital modifications as an impulse at pericentre while in chain regularization this procedure requires more care (Aarseth 2003a). Likewise, hyperbolic capture of neutron stars or point-mass particles by gravitational gravitation (cf. equation (15)) would require a similar treatment and may be worth the effort.

Issues connected with a larger length-scale should also be addressed. From equation (7) and the definition of  $c$  we have  $\tau_{\text{GR}} \propto r_h^{5/2}$  in  $N$ -body units for the same semi-major axis and eccentricity. Hence the two-body elements need to be more favourable in order for the GR regime to be reached with a comparable effort. Increasing the half-mass radii of the white dwarf cluster models indicates that relativistic effects may still be appreciable. Further explorations of such models are therefore desirable.

The intriguing question of the relative importance of resonant relaxation (Rauch & Tremaine 1996) versus Kozai cycles needs to be investigated. Other authors have pointed to the connection (Hopman & Alexander 2006) and, as reported above, there is no doubt that the latter process plays a crucial role triggering the early energy loss. Typical examples have been identified showing extreme eccentricity evolution for long-lived configurations with semi-major axis ratio of about 10. Even so, the actual duration may well be too short to be resolved by the present plotting procedure in some cases. As for de-tuning of the Kozai cycle, characteristic values  $\Delta\omega \simeq 0.05$  are obtained from equation (14) for the first-order precession during critical stages involving white dwarfs and this may not be excessive.

The importance of Kozai cycles in  $N$ -body simulations has been emphasized before (Iwasawa et al. 2006). In this work, the interaction of three massive objects ( $m_{\text{BH}} = 0.01$ ) in a system of  $N \simeq 10^5$  low-mass particles included the gravitational radiation term with fairly small values of  $c$ . The formation of hierarchical triples involving the three massive bodies frequently led to the ejection of one member by the sling-shot mechanism or, alternatively, to coalescence of the inner binary. The corresponding eccentricity displayed large and small spikes which is characteristic of Kozai cycles. As demonstrated above, including the GR precession does not suppress the eccentricity spikes. Given the enhanced precession rates during the approach to GR conditions, more work is needed to clarify this behaviour. In this connection, we note that the predicted maximum eccentricity is often reached before triggering the final stages leading to coalescence or tidal disruption.

It is interesting to compare the numerical challenges of studying one or two massive objects in a stellar system. In the latter case, the binary acts to clear the inner region by ejecting stars. The depletion of short periods therefore makes for an easier technical problem, provided a reliable method is available to deal with the massive binary Mikkola & Aarseth 2002, Aarseth 2003b). In either case quite large eccentricities are required for GR effects to manifest themselves. As far as the study of a single BH object is concerned, the wheel-spoke formulation provides a practical scheme for including post-Newtonian terms in a direct  $N$ -body code.

Applications to a star cluster model containing white dwarfs also show that significant orbital shrinkage by energy radiation loss is possible before disruption. Moreover, high eccentricities by the Kozai mechanism can still be achieved. These processes lead to an enhanced rate of swallowing by the BH but more extensive simulations are needed before the growth rate can be determined. Hence

the present software development provides a powerful tool for exploring both idealized and realistic problems of current interest. It remains to be seen whether such systems would bear any imprints of the swallowing process in the form of supernova events caused by white dwarf detonation (Dearborn, Wilson & Mathews 2005). Finally, the purpose of the present work is to present a viable new method, together with some results illustrating its capability. Hopefully, future work will address issues relating to time-scales and model dependence.

## 7 ACKNOWLEDGEMENTS

Much of the code refinements were done during a one month visit to the National Astronomical Observatory, Japan, when a draft was also produced. The author would like to thank Professor Eiichiro Kokubo for his kind hospitality. This visit was sponsored by the “GRAPE-DR Project” grant provided by MEXT, Japan. It is a pleasure to thank Seppo Mikkola for technical assistance. Discussions with Pau Amaro-Seoane and Rosemary Mardling clarified my understanding of GR implementations and few-body dynamics, respectively.

## REFERENCES

- Aarseth S.J., Gravitational N-Body Simulations, Cambridge Univ. Press, Cambridge
- Aarseth S.J., 2003b, Ap&SS, 285, 367
- Aarseth S.J., Zare K., 1974, Cel. Mech., 10, 185
- Alexander M.E., 1986, J. Comp. Phys., 64, 195
- Amaro-Seoane P., Freitag M., 2006, MNRAS, xxx, yyy
- Baumgardt H., Hopman C., Portegies Zwart S., Makino J., 2006, MNRAS, 372, 467
- Baumgardt H., Makino J., Ebisuzaki T., 2004, ApJ, 613, 1133
- Berczik P., Merritt D., Spurzem R., Bischof H., 2006, ApJ, 642, L21
- Blanchet L., Iyer B., 2003, Class. Quant. Grav., 20, 755
- Bulirsch R., Stoer J., 1966, Num. Math., 8, 1
- Dearborn D.S.P., Wilson J.R., Mathews G.J., 2005, ApJ, 630, 309
- Heggie D.C., 1996, private communication
- Hopman C., Alexander T., 2006, ApJ, 645, 1152
- Iwasawa M., Funato Y., Makino J., 2006, ApJ, 651, 1059
- Kozai Y., 1962, AJ, 67, 591
- Kupi G., Amaro-Seoane P., Spurzem R., 2006, MNRAS, 371, L45
- Lee M.H., 1993, ApJ, 418, 147
- Magorrian J., Tremaine S., 1999, MNRAS, 309, 447
- Makino J., 1991, ApJ, 369, 200
- Mardling R.A., Aarseth S.J., 2001, MNRAS, 321, 398
- Mikkola S., Aarseth S.J., 1993, Celes. Mech. Dyn. Ast., 57, 439
- Mikkola S., Aarseth S.J., 2002, Celes. Mech. Dyn. Ast., 84, 343
- Milosavlević M., Merritt D., 2001, ApJ, 563, 34
- Mora T., Will C., 2003, gr-qc/0312082
- Peters P.C., 1964, Phys. Rev., 136, B1222
- Preto M., Merritt D., Spurzem R., 2004, ApJ, 613, L109
- Quinlan G.D., Shapiro S.L., 1989, ApJ, 343, 725
- Rauch K.P., Tremaine S., 1996, New Astron., 1, 149
- Szell A., Merritt D., Mikkola S., 2005, in Buchler, J.R., Gottschman S.T., Mahon M.E. eds, Nonlinear Dynamics in Astronomy and Physics, Ann. New York Acad. Sci., 1045, 225
- Zare K., 1974, Celes. Mech., 10, 207
- Zhao H., 1996, MNRAS, 278, 488